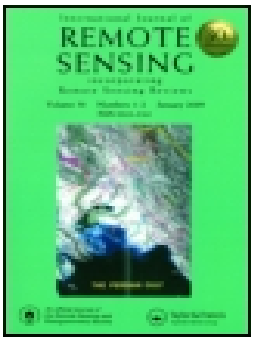

International Journal of Remote Sensing

ISSN: 0143-1161 (Print) 1366-5901 (Online) Journal homepage: http://www.tandfonline.com/loi/tres20

Impacts of land use and socioeconomic patterns on urban heat Island

Junmei Tang, Liping Di, Jingfeng Xiao, Dengsheng Lu & Yuyu Zhou

To cite this article: Junmei Tang, Liping Di, Jingfeng Xiao, Dengsheng Lu & Yuyu Zhou (2017) Impacts of land use and socioeconomic patterns on urban heat Island, International Journal of Remote Sensing, 38:11, 3445-3465, DOI: 10.1080/01431161.2017.1295485

To link to this article: http://dx.doi.org/10.1080/01431161.2017.1295485

Published online: 21 Mar 2017.

INTERNATIONAL JOURNAL OF REMOTE SENSING, 2017
VOL. 38, NO. 11, 3445–3465
http://dx.doi.org/10.1080/01431161.2017.1295485

Impacts of land use and socioeconomic patterns on urban heat Island

Junmei Tang[a], Liping Di[a], Jingfeng Xiao[b], Dengsheng Lu[c] and Yuyu Zhou[d]

[a]Center for Spatial Information Science and Systems, George Mason University, Fairfax, VA, USA; [b]Earth Systems Research Center, Institute for the Study of Earth, Oceans, and Space, University of New Hampshire, Durham, NH, USA; [c]Center for Global Change and Earth Observations, Michigan State University, East Lansing, MI, USA; [d]Department of Geological and Atmospheric Sciences, Iowa State University, Ames, IA, USA

ABSTRACT

Intensive land surface change and human activities induced by rapid urbanization are the major causes of the urban heat island (UHI) phenomenon. In this article, we examined the spatial variability of UHI and its relationships with land use and socioeconomic patterns in the Baltimore–DC metropolitan area. Census data, road network as well the digital elevation model (DEM) and average water surface percentage were selected to analyse the correlation between spatial patterns of UHI and socioeconomic factors. The impervious surface (coefficient of determination R^2 = 0.89) and normalized difference vegetation index (R^2 = 0.81) were the two most important landscape factors, and population density (R^2 = 0.57) was the most influential socioeconomic variable in contributing to the UHI intensity. Generally, the socioeconomic variables had smaller influence on the UHI intensity than the landscape variables. Based on the patch analysis, most of the socioeconomic variables influenced the UHI intensity indirectly through changing the physical environment (e.g. impervious surface or forest cover). The selected landscape and socioeconomic variables, except impervious surface percentage, demonstrated third-order polynomial correlation with the UHI intensity. The higher correlations were found within certain ranges such as forest percentage from 0% to 30% and population density from 0 to 5000 km^{-2}. This research provides a case study to understand the urban land surface, vegetation, and microclimate for urban management and planning.

ARTICLE HISTORY
Received 23 June 2016
Accepted 4 February 2017

1. Introduction

Rapid urbanization, triggered by the population growth and migration from rural to urban areas, is one of the most important phenomena from the beginning of the twenty-first century (Dale 1997; Rogers and McCarty 2000). Since the 1990s, more than 75% of the US population has resided in urban areas covering only about 3% of the US land area (US Census 2011). It has been widely recognized that the magnitude and

CONTACT Junmei Tang jtang8@gmu.edu Center for Spatial Information Science and Systems, George Mason University, Fairfax, VA 22030, USA

intensity of urbanization have produced profound impacts on our living environment including the hydrological cycle, biogeochemical cycle, and the climate system (Kalnay and Cai 2003; Ricketts and Imhoff 2003; Bounoua et al. 2009; Creutzig et al. 2015; Oleson et al. 2015). As urbanization accelerates globally and more than half of the world's population is living in cities, it is importance to quantify and monitor the complex interactions between the changing local environment and rapid urbanization associated with evolving socioeconomic development (Chapin III 2008; Tang, Wang, and Yao 2008).

Urban heat island (UHI) is considered as one of the conspicuous problems resulting from urbanization and human civilization in the twenty-first century (Rizwan, Dennis, and Liu 2008; Imhoff et al. 2010). The typical land-use/land-cover change induced by urbanization as converting natural vegetation and agricultural lands to impervious surfaces, along with the increasing anthropogenic heat release, modify urban local temperature and generate higher temperatures in urban areas than the surrounding rural areas (Carlson and Arthur 2000; Arnfield 2003; Wilby 2008; Bounoua et al. 2009). After discovered by Howard (1883) and defined by Manley (1958), the UHI has been broadly studied for decades in its spatial distribution patterns (Gallo et al. 1999; Xu and Chen 2004; Hart and Sailor 2009), daily-night dynamics (Giridharan, Ganesan, and Lau 2004; Schrijvers et al. 2015), seasonal variation (Gallo and Owen 1999; Yuan and Bauer 2007; Tomlinson et al. 2012), and temporal dynamics (Streutket 2003; Xu and Chen 2004; Wang et al. 2015).

The determinants and causative factors of the UHI have been much less studied than its spatial variability (Voogt and Oke 2003; Pu et al. 2006; Jenerette et al. 2007). Much emphasis has been placed on the correlation between thermal pattern and urban land-use land-cover pattern such as urban forest (Gallo et al. 1993; Weng, Lu, and Schubring 2004; Imhoff et al. 2010), impervious surface (Arnfield 2003; Xian et al. 2006; Zhang, Zhong, and Wang 2009; Guo et al. 2015), and water area (Chen, Zhao, Li, 2006; Livesley, McPherson, and Calfapietra 2016). For example, a negative relationship between thermal pattern and the satellite-derived normalized difference vegetation index (NDVI) has been extensively reported after the first exploration by Gallo et al. (1993). Besides the NDVI, other satellite-derived indices such as normalized different building index (NDBI) (Chen et al. 2006), normalized different water index (NDWI), and normalized different moisture index (NDWI) (Gao 1996) have been developed and correlated with the land surface temperature (LST). Fraction vegetation cover, which was less influenced by seasonal variations than the NDVI, has slightly stronger negative correlation with urban LST (Carlson, Gillies, and Perry 1994; Gutman and Ignatov 1998; Weng, Lu, and Schubring 2004; Mathew et al. 2015). Another commonly studied factor is impervious surface area (Xian and Crane 2006; Guo et al. 2015). Compared to the rural surroundings, impervious areas of cities differ considerably in albedo, thermal capacity, roughness, which modifies the surface energy budget and LST in highly urbanized areas (Giridharan, Ganesan, and Lau 2004; Hart and Sailor 2009; Weng, Rajasekar, and Hu 2011).

Anthropogenic heat released by human activities is another major source of UHI (Zhou et al. 2012). It has been investigated through the correlation between the spatial variations in surface temperatures and socioeconomic patterns such as population density, industrial production, and household income. Buyantuyev and Wu (2010) found the high correlation between daytime temperatures and median family income. Jenerette et al. (2007) found that the surface temperature on an early summer day in

Phoenix would decrease 0.28°C as neighbourhood annual median household income increased by \$10,000. Other related socioeconomic variables, such as electricity consumption and traffic of vehicles have been explored as socioeconomic drivers of urban heat island (Chen, Li, and Li 2003; Yue, Xu, and Xu 2010). The spatial pattern of UHI within a city is usually the combined results of both physical environment and land-use change caused by socioeconomic development (Wilson et al. 2003; Guo et al. 2015), therefore, a simple correlation analysis between single factor and thermal pattern is not enough to comprehensively understand the formation and development of UHI (Pu et al. 2006, Wang et al. 2015). Therefore, it is critical to investigate the spatial variation of UHI, land use, and socioeconomic patterns and to analyse the major driving forces behind these variations for a better understanding of the urban thermal environment.

In this study, we examined the relationships between the spatial variation of urban heat island, land use, and socioeconomic patterns in the Baltimore–DC Metropolitan Area. The specific research questions are twofold: (1) what is the spatial pattern of LST and UHI intensity at Baltimore–DC area and can the LST and UHI intensity be interpreted on the basis of Landsat TM imagery? (2) Which land-use change or socioeconomic factor has a more significant effect to the UHI and how they correlate with the spatial pattern of UHI intensity? The UHI intensity, defined as the temperature difference (ΔT) between urban, suburban and exurban locations (Tan et al. 2010), was used to evaluate the spatial distribution of UHI at the study area. We combined the remote-sensing-derived UHI intensity with the physical environment and socioeconomic status to examine the direct and indirect causes of UHI. Fourteen variables were selected to represent the land use and socioeconomic patterns. The examination of the relationships between UHI intensity, land use, and socioeconomic patterns will help us examine the spatial variation of UHI and understand the physical impact and indirect impact from social drivers on UHI patterns.

2. Data and methods

2.1. *Study area*

Our study area is the Baltimore–DC metropolitan area (Figure 1) covering an area around 14,000 km^2. Centred at 76° 46′ W and 39° 18′ N, this area makes up less than 6% of the Chesapeake Bay watershed but accounts for over 45% of its total population (Dougherty et al. 2004). As one of the nation's fastest growing regions, the Baltimore–DC metropolitan area has experienced rapid economic development and population growth since 1950 with more than 8 million residents in 2010 (U S Census 2011). The increasing megalopolis patterns have modified the percentages in wetland, forest, and agriculture ecosystems (Foresman, Pickett, and Zipperer 1997) and changed the local thermal patterns (Figure 2). This trend has been extended for more than 30 years, eliciting concern as early as the 1960s about emerging trends related to socioeconomic development and urban environment degradation (Von Eckardt and Gottman 1964).

The Baltimore–DC metropolitan area is a representative coupled natural-human ecosystems in the USA, and has a unique role in economics, politics, and cultural activities (Lamptey, Barron, and Pollard 2005). The rapid land surface change with a stable population growth led to regional climate change, strengthening the heat corridor along the Baltimore–DC area (Viterito 1989). The increasing surface temperature

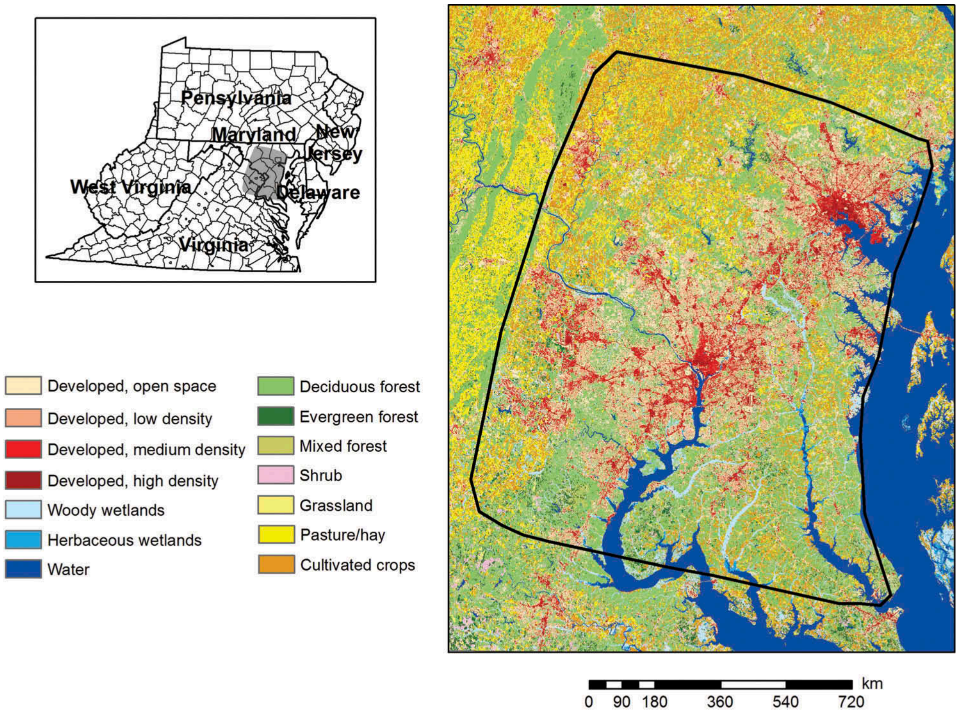

Figure 1. Location and land-use land-cover map of the study area.

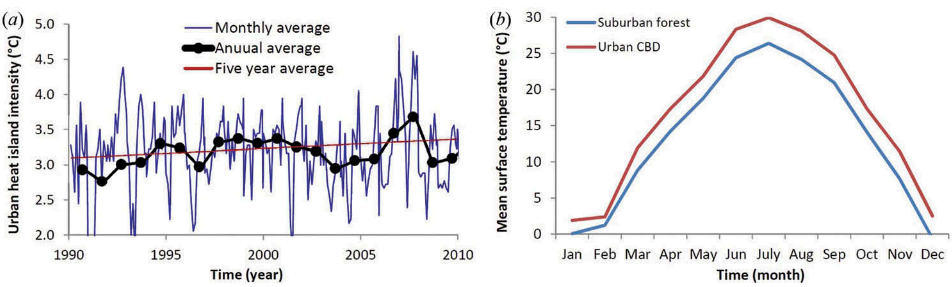

Figure 2. (a) The monthly/yearly change of UHI intensity from 1990 to 2010; and (b) monthly pattern in Baltimore–DC metropolitan area. Note: the UHI intensity was derived from the temperature difference between downtown station and rural station in Baltimore.

difference between the weather stations in the downtown area and those in the rural area in recent years has confirmed the UHI phenomenon in our study area (Baltimore region as an example in Figure 2).

2.2. *Data*

We combined several data sources including Landsat Thematic Mapper (TM) imagery, census data, road network, and digital elevation model (DEM) to examine the patterns of UHI, land-use, and socioeconomic factors and their relationships. The Landsat TM imagery was used to derive surface temperature and land-use patterns. A subset image from Landsat TM acquired on 22 August 2010 was used in this study. The conventional Maximum Likelihood Classification (MLC) was performed to classify the land use/land cover into residential, commercial/industrial, forest, grassland, barren land, cropland, wetland, and water. The US census data were used to derive socioeconomic variables. Socioeconomic variables, including population density, average age, median income, unemployment rate, year of house built, number of households, and family size were collected from the 2010 decennial US Census for all 1540 census tracts in the Baltimore–DC metropolitan area. These socioeconomic variables were selected to represent distinct socioeconomic characteristics of demographic status, settlement age, family size, employment condition, respectively. We also used the Environmental Systems Research Institute's (ESRI's) GIS road network to derive road density. DEM data with 30 m spatial resolution were obtained from USDA Data Gateway (USDA 2015). DEM data was used to derive terrain pattern such as elevation and slope.

All the images, ESRI data, and census data were registered/reprojected to UTM coordinate system (WGS 84, Zone 18) with root mean squared error (RMSE) of less than 15 m.

2.3. *Estimation of LST and UHI intensity from Landsat TM imagery*

The Landsat TM thermal infrared band (10.4–12.5 μm) was utilized to derive LST and UHI intensity. The digital numbers (DNs) of the infrared band was converted to at-satellite brightness temperature (i.e. blackbody temperature, T_B) with the hypothesis of uniform emissivity (Landsat Project Science Office 2002; Chander and Markham 2003) using the following equation:

$$T_B = \frac{K_2}{\ln\left(\frac{K_1}{L_\lambda} + 1\right)} \tag{1}$$

with

$$L_\lambda = \frac{L_{max} - L_{min}}{Q_{max} - Q_{min}}(DN - Q_{min}) + L_{min}, \tag{2}$$

where T_B is the effective at-satellite temperature in K; K_1 (=607.76 W m^{-2} sr^{-1} μm^{-1}) and K_2 (=1260.56 K) are pre-launch calibration constants; L_λ in W m^{-2} sr^{-1} μm^{-1}) is the spectral radiance or top-of-atmospheric (TOA) radiance measured by the Landsat sensor; Q_{max} and Q_{min} are the minimum (=0) and maximum (=255) DN values; L_{max} and L_{min} are the detected spectral radiance that are scaled to Q_{max} and Q_{min}; λ is the wavelength.

The blackbody temperature, T_B, was then converted to the temperature at the surface of nature land cover based on the spectral emissivity (ε) and the emissivity corrected LST (S_t) were derived as follows (Artis and Carnahan 1982):

$$S_t = \frac{T_B}{1 + (\lambda T_B/\rho)\ln\varepsilon} \text{ with } \rho = hc/\sigma, \tag{3}$$

where λ is the wavelength of emitted radiance, for which the peak response of average limiting wavelengths (λ = 11.5 μm) (Markham and Barker 1985); σ is the Boltzmann constant (1.38×10^{-23} J K^{-1}), h is the Planck's constant (6.626×10^{-34} J s), and c is the velocity of light (2.998×10^8 m s^{-1}); ε is the target-specific surface emissivity which were assigned based on our land-cover categories and emissivity values from Snyder et al. (1998).

We examined the characteristics of the UHI intensity using the temperature difference between the studied location and rural areas and compared the UHI among census tract. First, the rural temperatures were derived by masking out all areas of clouds, open water and urban or build up pixels. A mean planar surface was used to fit the 'rural' pixels to determine the rural temperature (T_r), leaving only the heat island signature. We used the temperature difference (ΔT) between the urban and build-up cells (T_s) and rural planar surface (T_r) to measure the UHI intensity:

$$\Delta T(i,j) = T_s(i,j) - T_r, \tag{4}$$

where $T_s(i,j)$ is the LST of the land-cover type of urban and built-up at location (i, j), T_r is the rural temperature normalized from the non-urban pixels.

2.4. *Fraction maps derived from spectral mixture analysis and aggregation*

Linear spectral mixture analysis (LSMA), one of most widely used sub-pixel classification methods, was used to estimate the sub-pixel proportions of impervious surface in urban environments (Lu et al. 2014; Tang, Wang, and Myint 2007; Weng, Lu, and Schubring 2004; Wu and Murray 2003). The LSMA has so far been the most popular approach in the SMA family methods given its simple mathematical form (Adams et al. 1995; Cochrane and Souza 1998; Roberts et al. 1998; Singer and McCord 1979):

$$R_n = \sum_{e=1}^{E} r_{n,e} f_e + \varepsilon_n \text{ with} \sum_{e=1}^{E} f_e = 1 \text{ and } 0 \le f_e \le 1, \tag{5}$$

where R_n is the normalized spectral reflectance after MNF-transformation for each band n; f_e is the fraction of endmember e; E is the total number of endmembers; $r_{n,e}$ denotes the normalized spectral reflectance of endmember e within a pure pixel on band n; and ε_n is the residual error.

Based on the aerial photo of the study area, we selected four endmembers for the study area: high-albedo, low-albedo, vegetation, and soil. This four-endmember SMA was applied to each pixel and the best endmember combination was automatically chosen when the RMS ($\mathrm{RMS} = \sqrt{\frac{\sum_{n=1}^{M} (\varepsilon_n)^2}{M}}$) was minimized with a reasonable fraction (fractions between 0% and 100%) for each endmember class. For each grid cell, the high albedo and low-albedo were merged to represent the impervious surface percentage.

We aggregated the forest pixels and water pixels of the land-cover map derived from the MLC method to the census tract level to calculate the percentages of forest cover and water cover. Road maps were overlapped with the census tract map and road density was calculated by dividing total road length by the land area of each census tract. We used the percentages of impervious surface, forest, and water, other three landscape indicators (NDVI, elevation, and slope), and seven socioeconomic variables (population density, medium income, number of households, medium age, house age, family size, and unemployment rate) to investigate the impact of land use and socioeconomic patterns on UHI. These socioeconomic variables were selected to represent the distinct household characteristics to stand for their socioeconomic status, including demographic characteristics, living condition, and economic status.

2.5. *Statistical correlation analysis by Pearson's correlation and path analysis*

The statistical correlation analysis consisted of independent Pearson's correlation between the UHI intensity and the selected variables of land use/socioeconomic pattern. We first used the linear regression and Pearson's correlation to evaluate the relationship between UHI and each variable. To further identify the interactions among UHI, landscape, and socioeconomic variables, a multivariate analysis based on the path analysis model was used (Joreskog and Sorbom 1993; Akintunde 2012) to measure the direct effects of land use and socioeconomic variables on UHI, the direct effects of socioeconomic variable on land use, and the indirect effects of the socioeconomic variables on UHI through their influences on land use. Most of UHI studies selected the several significant variables without considering the indirect impacts from other variables. For example, impervious surface is highly related to UHI, while the population density has much less impact on UHI through changing impervious surface. In fact, population density increasing could exert influences on UHI through building more houses, paving the roads and parking lots which increase impervious surface area. There has been limited research on the contribution from less significant variables although these variables are highly related to the significant ones.

We used path analysis to examine the direct and indirect effects of the landscape and socioeconomic variables on UHI. Path analysis is one of the statistical methods to analyse multiple dependent and independent variables (Jenerette et al. 2007) and to measure the effects from dominant variables and insignificant ones. As a natural extension of regression analysis, path analysis method is a decision support tool that can quantify the direct contributions to the UHI and indirect effects through other variables to the UHI (Akintunde 2012). In this study, we first standardized all variables as follows:

$$Z = \frac{X - \mu}{\sigma}, \tag{6}$$

where μ is mean and σ is standard deviation. The linear regression analysis was then used to derive the impact coefficient of each independent variable i on the UHI. The independent variables included the selected 14 landscape and socioeconomic variables. These direct impact coefficients, together with the correlation matrix (M) between two variables, were used as partial regression coefficients to derive the indirect impact of each variable. The total effect $E(X_i, U)$ from any variable X_i to UHI intensity were calculated as

$$\begin{aligned} E(X_i, U) = D_E(X_i, U) + D_E(X_1, U) \times M(i, 1) + D_E(X_2, U) \times M(i, 2) + \cdots + D_E(X_n, U) \\ \times M(i, n), \end{aligned} \tag{7}$$

where $E(X_i,U)$ and $D_E(X_i,U)$ are the total impact and direct impact coefficients from variable i to UHI and $M(i,n)$ is the correlation index between variable i and variable n.

3. Results and discussion

3.1. *Spatial distribution of UHI intensity*

Figure 3 shows the Landsat-derived LST with the distribution of large populated areas within the Baltimore–Washington metropolitan area. The LST ranges from 281.5 to 320.2 K with a mean of 299.4 K and standard deviation of 3.3 K. The choropleth map (Figure 3) was produced based on the mean LST, indicating from minimum to Maximum LST increasing by standard deviation (Smith 1986; Weng, Lu, and Schubring 2004). High LST were identified extensively in the downtown areas of Baltimore and Washington DC, and in the surrounding cities around the Central Business District. Apparently, the eastern shore of the study area had larger LST than the western region which was largely covered by farmland and forest area. Several relatively large cities near Baltimore and Washington DC, such as Columbia, Silver Spring, Alexandria, and Arlington had higher LST than the nearby rural areas, and some cities in the forested region, such as Fredrick, Gaithersburg, and Dale City (population larger than 60,000), also had larger LST than nearby rural areas. Many high LST spots were found along the interstate highway 95 linking Baltimore and Washington DC and the state highway 270 linking DC and Fredrick.

3.2. *Correlation of UHI intensity with land use and socioeconomic patterns*

The thermal signature of each LULC type was examined to better understand the relationship between UHI and land use in the study area (Figure 4). It is clear that the commercial/industrial area exhibited the highest mean LST (305.0 K), followed by the

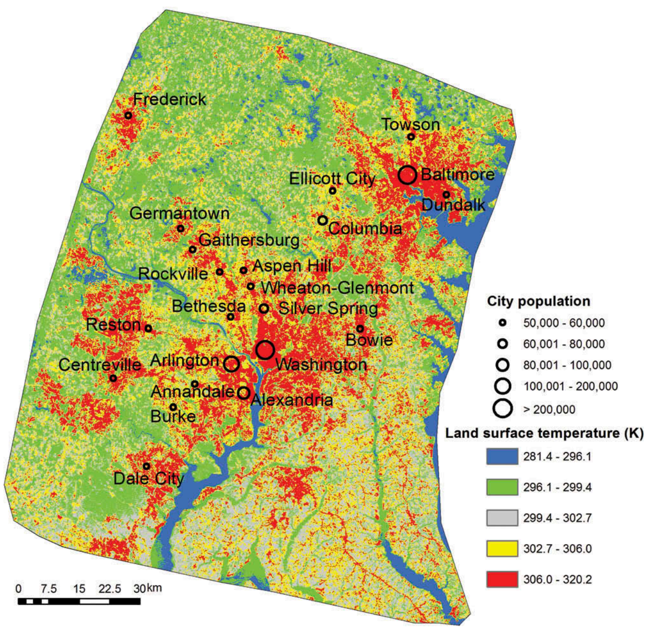

Figure 3. Spatial distribution of land surface temperature with city population.

residential area (301.5 K) and barren area (300.3 K). The natural surfaces had relatively similar mean LST, with the lowest temperature in water (295.4 K), wetland (297.9 K), and forest (298.3 K). This suggested that urban development increased the LST by at least 10 K by replacing the nature landscapes with non-transpiring, non-evaporating, and non-infiltrating surfaces. The large standard deviation value of LST in commercial/ industrial (2.26) and residential area (2.33) indicated that variation in these areas may be caused by the different construction materials and intensive human activities existing within these types of land use. Because of distinctive characteristics in urban areas, a further exploration on the spatial variation of LST caused by the land use and socio-economic pattern is necessary.

Figure 5(a–e) show the distribution of UHI intensity with four selected variables with two landscape variables – impervious surface and NDVI and two socioeconomic variables – population density and median income. There was a corresponding pattern between UHI intensity and impervious surface, especially in the Central Business District of Baltimore and DC. The higher similarity between UHI intensity and impervious surface indicates that impervious surface had higher correlation with UHI intensity than other variables and could be one important factor influencing the spatial distribution of UHI.

There was a small discrepancy between the UHI intensity and impervious surface maps in the southeastern corner covered by a high dense forest area with scattered houses (Figure 5(a–e)). Although this area had relatively a relatively low percentage of impervious surfaces, some high temperature areas in linear shapes were identified. This could be attributed to the high road density and the relatively high traffic volume between this area and the area downtown DC. The NDVI image showed low NDVI values in two urban centre areas corresponding with high UHI intensity; the lightest area (with the largest NDVI) is in the southern DC area corresponding to the Prince William Park and its surrounding areas and this highly forested area exhibited a small but extremely homogeneous low UHI intensity. The NDVI showed a clear, negative

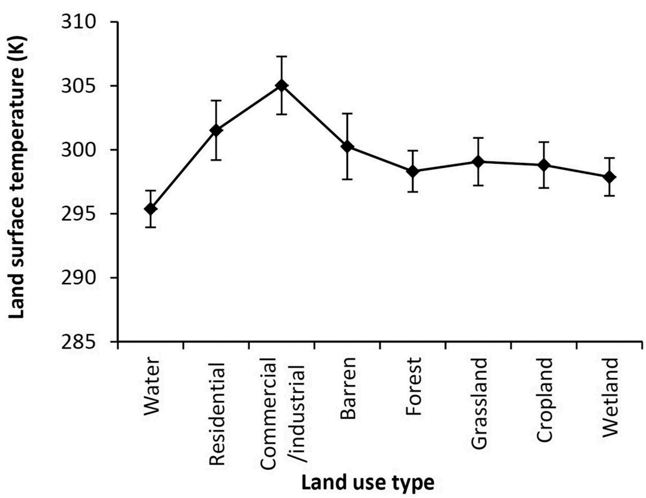

Figure 4. Mean land surface temperature of each land-use type with the error bar showing its standard deviation.

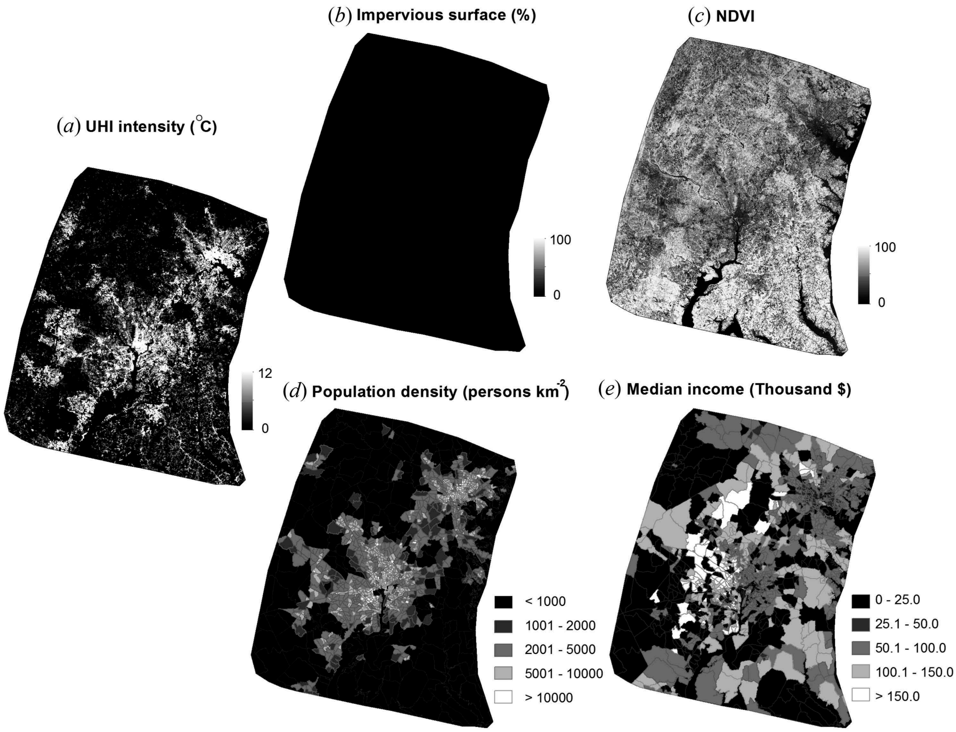

Figure 5. Patterns of selected biophysical and socioeconomic variables in Baltimore–DC metropolitan region: (a) spatial pattern of UHI intensity, increasing from 0°C to 12°C; (b) impervious surface in percentage (0–100%); (c) NDVI (0–1); (d) population density at census tract level (from 0 to 25,655 persons km^{-2}); and (e) median income ($9150 to $247,064).

relationship with the UHI intensity across nature and man-made land surfaces. These results are similar with the research reported by Li et al. (2011) and Guo et al. (2015) who studies the two largest cities, Shanghai and Guangzhou in China.

Compared to the physical land use, most socioeconomic variables showed lower correlation with the UHI intensity (Figure 5(a–e)). The most influential socioeconomic variable was population density which was highly correlated with the impervious surface area, showing an increasing pattern from suburban area to downtown area with increasing UHI intensity. Although most of high UHI intensity locations were associated with high density population centres, several high UHI intensity areas were located in the low population density areas, including the highway corridor connecting the military centres in the southeastern corner to the city of Waldorf and Saint Charles. The high UHI intensity in the low density population areas might be caused by the intensive traffic within these areas, indicating that road density and road use frequency should be considered in UHI studies. Median income had less correlation with UHI intensity than the population density although median income is one of important economic indicators for urbanization. The spatial variation of median income, with high values in the western and southwestern DC and low values in eastern DC, showed that there might be a slightly negative relationship between median income and the UHI intensity. These spatial patterns between UHI intensity and physical landscape and socioeconomic variables indicate that the spatial variation of UHI intensity was not driven by one of these variables alone, but by multiple variables. Some driving variables such as impervious surface and forest percentage affect UHI directly, while other variables such as population density and NDVI impact UHI indirectly though influencing other variables (Jenerette et al. 2007). Therefore, it is essential to further examine both direct and indirect effects of various driving factors on UHI intensity.

The relationships of UHI intensity with land use and socioeconomic patterns were examined through Pearson's correlation analysis at the census tract level (Table 1). The impervious surface and NDVI showed higher correlations with the UHI intensity compared to other variables. The strongest correlate was impervious surface, followed by NDVI and forest percentage. Other positive correlations included population density, road density, unemployment rate, and house age, while negative correlations included forest percentage, mean elevation, family size, median age, median income, mean elevation, and number of households. The variables related to urbanization such as impervious surface expanding and road construction and socioeconomic development could increase the UHI intensity. The variables improving the urban environment and the human wellbeing such as planting trees and increasing family income could decrease the UHI intensity. Most physical land use had relatively higher Pearson's correlation coefficient and are important factors controlling the distribution of the UHI intensity. Socioeconomic variables had relatively low coefficient of variation (mean = 0.62) than landscape variables (mean = 1.00). The lower difference in socioeconomic variables than landscape variables made them less detectable in influencing the UHI intensity. Although the direct impact of socioeconomic development is not as significant as that of land use, the interaction between land use and socioeconomic variables indicates that these influences could be created indirectly through changing the physical environment by intensive human activities.

Table 1. Descriptive statistics of land use, socioeconomic variables aggregated averagely on the census tract level and correlation with UHI intensity.

Variable	Minimum	Maximum	Mean (SD)	Coefficient of variation	Pearson's correlation
UHI intensity	0.03	8.57	2.78 (1.77)	0.64	
(a) Land use					
Impervious surface (%)	0.05	93.39	29.59 (20.67)	0.70	0.94
Mean NDVI	0.00	0.65	0.39 (0.13)	0.33	−0.89
Forest (%)	0.00	82.10	15.45 (15.52)	1.00	−0.71
Road density (km^{-1})	0.00	36.39	5.88 (4.67)	0.79	0.63
Mean elevation (m)	2.18	264.32	70.13 (46.27)	0.66	−0.44
Water (%)	0.00	20.94	0.49 (1.51)	3.08	−0.20
Slope (°)	0.48	11.27	3.28 (1.46)	0.45	−0.05
(b) Socioeconomic variable					
Population density (1000 persons km^{-2})	0.00	25.66	2.62 (2.36)	1.11	0.63
Unemployment (%)	0.00	57.10	7.05 (6.90)	0.98	0.40
House age	0	75	39 (25)	0.64	0.36
Family size	1	5	2.60 (0.44)	0.17	−0.28
Median age	17	77	36.29 (5.63)	0.16	−0.27
Median household income (thousand $)	0	247	64 (49)	0.77	−0.26
Number of households	0	6242	1681 (891)	0.53	−0.14

SD stands standard deviation.

The multivariate model was constructed and then the path analysis model was developed to investigate the direct and indirect effects of these variables on the UHI intensity. Table 2 summarizes the direct and indirect impacts of each variable. The impervious surface, population density, unemployment rate, family size, median age, and number of households were positively correlated with UHI intensity, while mean NDVI, forest percentage, road density, mean elevation, water percentage, slope, house age, and median income were negatively correlated with UHI intensity. Most variables had negative direct impact on the UHI intensity. Impervious surface had the highest direct impact (0.87), and its impact was much higher than the total effect of all negative factors. Mean NDVI, road density, forest percentage, and population density showed negligible negative direct impacts (–0.05 and –0.09) on the UHI intensity, they had relatively high indirect impact (–0.84 and 0.71) due to their high correlation with the impervious surface. Forest percentage (–0.62) and population density (0.62) had high indirect impacts and small direct impacts. Mean elevation, unemployment rate, and house age had moderate effects on UHI intensity (–0.44, 0.40, and 0.37), while the least correlation were found for water percentage (–0.20), number of households (–0.15), and slope (–0.06). These might be attributed to their small spatial variation among tracts (Table 1) and less correlation with impervious surface.

Figure 6 shows the detailed correlation of UHI intensity with its direct and indirect variables. The impervious surface explained 87% of direct impact on the spatial variation of UHI intensity, followed by mean elevation (10%), road density (9%) and forest percentage (8%). Other variables had small direct impacts and most of them showed indirect impact on the UHI intensity through influencing the impervious surface percentage. Among those variables, the mean NDVI (–0.89 total effect) and forest percentage (–0.71) were the two most important physical landscape variables, while the population density (0.67) and unemployment rate (0.39) were the two most important socioeconomic variables. The road density was also highly related to the UHI intensity (0.62)

Table 2. Total, direct, and indirect effects of landscape and socioeconomic patterns on UHI intensity.

Variable	Total effect on UHI intensity	Direct	Indirect
(a) Land use			
Impervious surface (%)	0.9396	0.8731	0.0665
Mean NDVI	−0.8892	−0.0450	−0.8442
Forest (%)	−0.7059	−0.0834	−0.6224
Road density (km^{-1})	0.6241	−0.0906	0.7147
Mean elevation (m)	−0.4400	−0.0942	−0.3457
Water (%)	−0.1965	−0.0283	−0.1683
Slope (°)	−0.0519	−0.0244	−0.0275
(b) Socioeconomic variables			
Population density (thousand km^{-2})	0.6240	0.0044	0.6196
Unemployment (%)	0.3983	0.0454	0.3529
House age	0.3694	−0.0014	0.3709
Family size	−0.2796	0.0879	−0.3675
Median age	−0.2637	0.0035	−0.2672
Median household income (thousand $)	−0.2426	−0.0035	−0.2391
Number of households	−0.1487	0.0169	−0.1656

The direct effect is the correlation between each variable and UHI intensity while the indirect effect is the combined impact index through impervious surface.

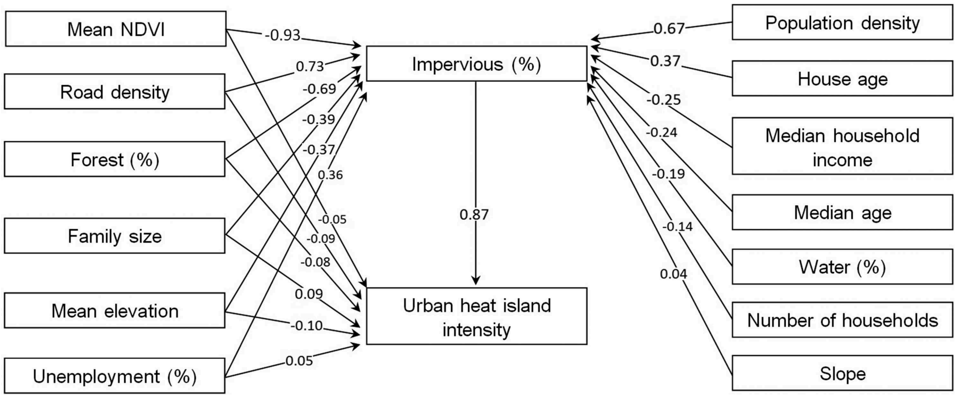

Figure 6. Path analysis results showing the determinants of UHI intensity. Note: the left part of figure shows the direct impact factors with regression coefficients larger than 0.05 and right part is the indirect impact factors through impervious surface.

mainly because road intensity was correlated with impervious surface (0.73). The least important variables were slope (–0.02) and number of households (0.02) and their total effect values (–0.05 and –0.15) were the lowest among all variables. The low correlation between UHI intensity, impervious surface, and number of household indicates that constructing housing itself is not the most significant reason causing the UHI while community development such as paving the road and constructing public buildings and parking lot which significantly increase the albedo and modify the radiation fluxes, increasing the UHI intensity in the Baltimore–DC area.

3.3. *Management implications for urban climate at local scale*

Urbanization is one of the most important components of global change and modifies the land surface, species diversity, and quality of human life (Hope et al. 2003; Jenerette et al. 2007). Improved understanding of urbanization induced local climate change will help us develop a more sustainable environment for rapidly growing urban areas. Within the Baltimore–DC metropolitan region, the UHI intensity was strongly related with the impervious surface (coefficient of determination R^2 = 0.89) and NDVI (R^2 = 0.81). Using bivariate linear regression analysis (Figure 7), we estimated the UHI intensity of census tract could increase by 0.45°C with every 10% increase of impervious surface percentage. Although most of the impervious surface within tracts ranged from 0% to 50%, a clear linear relationship was found between impervious surface and UHI intensity. The majority of mean NDVI values were between 0.3 and 0.6, showing a clear negative correlation with UHI intensity within this range. The tracts with NDVI smaller than 0.3 showed a weaker decreasing trend compared to the tracts with larger NDVI. This indicates that it is important to manage the area having medium to high vegetation cover since a small increase of NDVI in these areas could significantly reduce the UHI intensity. NDVI values were calculated based on all the types of vegetation. The spatial variation of NDVI can be influenced by many factors such as vegetation types, topography, slope, and solar radiation availability (Walsh et al. 1997). When we mitigate the urban micro-scale climate impact with the help of vegetation, we need to consider the planting location,

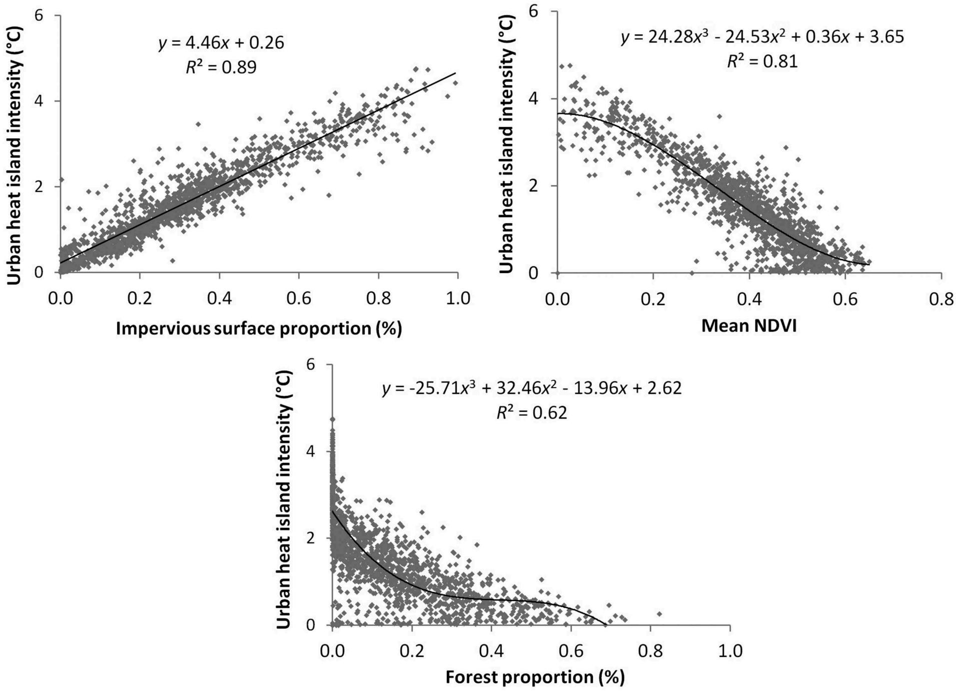

Figure 7. Scatter plots of bivariate relationship between UHI intensity and three most influential land-use variables.

vegetation type, the potential growth pattern as well as the neighbouring environment to improve its effectiveness. The strong correlation between forest percentage and UHI intensity (Table 2) indicates that forest could be the most important vegetation type for the mitigation of the UHI effects.

A closer look at the correlation between forest percentage and UHI intensity indicated that the relationship between vegetation and UHI was not linear in Baltimore–DC region. The forest percentage also showed negative correlation with the UHI intensity but different changing trend compared to NDVI. We found a dramatic decrease in the UHI intensity when the forest percentage increased from 0% to 30% and this pattern levelled off when the fraction increased to 40% or larger. This indicates that planting trees could significantly reduce the UHI intensity and improve the local urban climate in the high density build-up area. However, in the high density forest area (forest percentage >50%), the tree cover could be less important than other landscape or socioeconomic for controlling UHI variables.

Figure 8 shows the bivariate relationship between UHI intensity and three most influential socioeconomic variables. Both increasing population density and unemployment rate could increase the UHI intensity positively, especially in the low value ranges. The highest correlations between population density and UHI intensity were found in the tracts with population density from 0 to 5000 persons km^{-2}, with the correlation levelling off in the tracts with population density higher than 10,000 persons km^{-2}. There are two possible reasons: (1) the number of census tracts with high population density (>1000 persons km^{-2}) was low; and (2) most of these high density tracts were distributed between the downtown area and suburban areas. The cooling effect from the neighbouring suburban area could reduce the UHI intensity

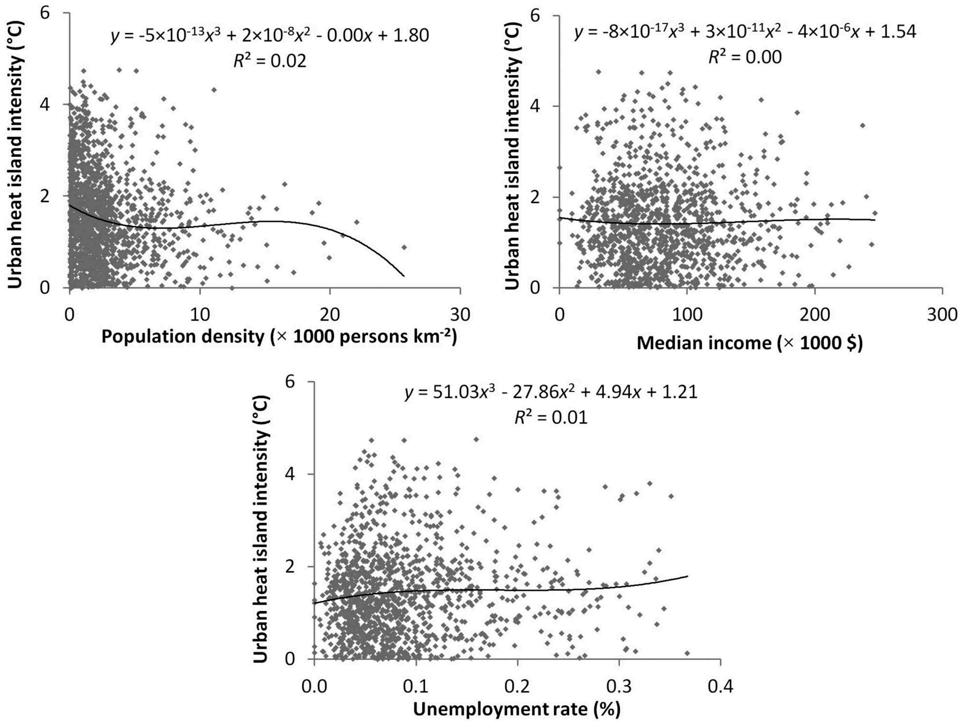

Figure 8. Scatter plots of bivariate relationship between UHI intensity and three most influential socioeconomic variables.

in this area. The median income showed relatively clear negative correlation with UHI intensity when median income ranged from \$0 to \$100,000, and their relationship was weaker when median income exceeded \$150,000. These high income tracts (median income > \$150,000) are located in the western Baltimore and DC area with low impervious surface percentage (average percentage = 12%) and high forest coverage (average percentage = 28%). Increasing the unemployment rate could slightly increase the UHI intensity, especially for the tracts with an unemployment rate between 10% and 20%. Most of the tracts with very high unemployment rate are located either in downtown Baltimore or eastern DC area with high UHI intensity (average = 2.6°C). The tracts with high unemployment rate but low UHI intensity either had high forest coverage (forest coverage 28% with UHI intensity 0.7°C) or had high NDVI (mean NDVI 0.39 with UHI intensity 1.3°C). All selected variables had some correlation, to a higher or lower degree, with the UHI intensity which further indicates that the UHI intensity was influenced by multiple variables and these variables affect each other through direct or indirect impacts. To implement the urban planning to mitigate the UHI phenomenon, we need to consider not only the landscape pattern and socioeconomic variables but also their interactions.

4. Conclusions

This study explored the spatial variation of LST and UHI intensity in the Baltimore–DC metropolitan area and investigated the relationships between UHI, land use, and socioeconomic patterns. Most of high LST locations were found in the downtown urban area of Baltimore and DC, with several small UHI hot spots in the suburban areas. The impervious surfaces, especially the commercial/industrial areas with intensive human activities in the downtown area, exhibit the strongest UHI intensity and highest LST. The results indicate that UHI is a complex phenomenon and a single factor approach can hardly explain the UHI and its distribution. Among all the landscape indicators, the impervious surface and NDVI are the two most influential factors in determining the UHI intensity through the modification of radiation and evaporation patterns. The factors with least impact are water percentage and slope.

The socioeconomic patterns show less important impact on the UHI intensity compared to the land use; meanwhile, socioeconomic factors have indirect impacts on UHI intensity through changing the percentage of the impervious surfaces. The highest influential socioeconomic factor is population density due to its high correlation with impervious surface. Other socioeconomic variables such as unemployment rate, house built year, and median income, show low correlation with impervious surface and little impact on the UHI intensity. With the evaluation of land use and socioeconomic patterns, we found that fast socioeconomic development areas are always correlated with high percentages of impervious surface, and therefore, high mean surface temperature and high UHI intensity. However, when socioeconomic development reaches a certain level, such as the census tracts with high median income and small number of households, it usually associates with low impervious surface and high vegetation cover. These areas are usually found in the suburban or rural-to-urban transition area as impervious surface and population are low with a decreased intensity of the UHI phenomenon.

This research extended the traditional UHI research by addressing multiple UHI contributing factors including both landscape and socioeconomic variables using a path analysis model. While the spatial variation in the UHI has been studied and many impact variables, such as vegetation cover, impervious surface, have been investigated previously, our analysis examined comprehensive mechanisms by analysing the spatial variability of LST and UHI intensity for a heterogeneous region and selecting multiple driving variables. These results enhanced previous studies in three ways. First, compared to previous UHI studies focusing on one or two impact factors, we selected a comprehensive set of land use and socioeconomic factors to investigate the social-ecological-climate correlation in a highly urbanized area. Second, previous research focused on the direct impact, this study extended the concept to the direct and indirect impact using a path analysis model by treating the urban as one ecosystem. Third, our study provided a case study for more specific questions in urban microclimate such as how to fully understand the well-established relationships between land surface, vegetation, and microclimate (Hanamean et al. 2003; Smith and Johnson 2004) and how to implement these results in urban management and planning. The further steps for this study will be multiple year and inter-annual change of spatial pattern of the UHI and how these relationships vary through time in seasonal cycle and inter-annual change. Further exploration on these questions will help us to differentiate the impact of each variable and better understand the physical and socioeconomic causes of UHI to develop more sustainable urban environments.

Acknowledgements

This study was supported by the National Aeronautics and Space Administration (NASA) through the Carbon Cycle Science Programme (award number NNX14AJ18G) and National Science Foundation (NSF) through Earthcube Programme (award number ICER-1440294). It was also partly supported by NASA through the Science of Terra and Aqua (award number NNX14AI70G).

Disclosure statement

No potential conflict of interest was reported by the authors.

Funding

This study was supported by the National Aeronautics and Space Administration (NASA) through the Carbon Cycle Science Programme (award number NNX14AJ18G) and National Science Foundation (NSF) through Earthcube Programme (award number ICER-1440294). It was also partly supported by NASA through the Science of Terra and Aqua (award number NNX14AI70G).

ORCID

Yuyu Zhou http://orcid.org/0000-0003-1765-6789

References

Adams, J. B., D. E. Sabol, V. Kapos, R. A. Filho, D. A. Roberts, M. O. Smith, and A. R. Gillespie. 1995. "Classification of Multispectral Images Based on Fractions of Endmembers: Application to Land Cover Change in the Brazilian Amazon." *Remote Sensing of Environment* 52: 137–154. doi:10.1016/0034-4257(94)00098-8.

Akintunde, A. N. 2012. "Path Analysis Step by Step Using Excel." *Journal of Technical Science and Technologies* 1: 9–15.

Arnfield, A. J. 2003. "Two Decades of Urban Climate Research: A Review of Turbulence, Exchanges of Energy and Water, and the Urban Heat Island." *Internal Journal of Climatology* 23: 1–26. doi:10.1002/joc.859.

Artis, D. A., and W. H. Carnahan. 1982. "Survey of Emissivity Variability in Thermography of Urban Areas." *Remote Sensing of Environment* 12: 313–329. doi:10.1016/0034-4257(82)90043-8.

Bounoua, L., A. Safia, J. Masek, C. Peters-Lidard, and M. L. Imhoff. 2009. "Impact of Urban Growth on Surface Climate: A Case Study in Oran, Algeria." *Journal of Applied Meteorology and Climatology* 48: 217–231. doi:10.1175/2008JAMC2044.1.

Buyantuyev, A., and J. Wu. 2010. "Urban Heat Islands and Landscape Heterogeneity: Linking Spatiotemporal Variations in Surface Temperatures to Land-Cover and Socioeconomic Patterns." *Landscape Ecology* 25: 17–33. doi:10.1007/s10980-009-9402-4.

Carlson, T. N., and S. T. Arthur. 2000. "The Impact of Land Use-Land Cover Changes Due to Urbanization on Surface Microclimate and Hydrology: A Satellite Perspective." *Global Planet Change* 25: 49–65. doi:10.1016/S0921-8181(00)00021-7.

Carlson, T. N., R. R. Gillies, and E. M. Perry. 1994. "A Method to Make Use of Thermal Infrared Temperature and NDVI Measurements to Infer Surface Soil Water Content and Fractional Vegetation Cover." *Remote Sensing Review* 9: 161–173. doi:10.1080/02757259409532220.

Chander, G., and B. Markham. 2003. "Revised Landsat-5 TM Radiometric Calibration Procedures and Postcalibration Dynamic Ranges." *IEEE Transactions on Geoscience and Remote Sensing* 41: 2674–2677. doi:10.1109/TGRS.2003.818464.

Chapin, F. S. III, J. T. Randerson, A. D. McGuire, J. A. Foley, and C. B. Field. 2008. "Changing Feedbacks in the Climate-Biosphere System." *Front Ecology Environment* 6: 313–320. doi:10.1890/080005.

Chen, X., H. Zhao, P. Li, and Z.-Y. Yin. 2006. "Remote Sensing Image-Based Analysis of the Relationship between Urban Heat Island and Land Use/Cover Changes." *Remote Sensing of Environment* 104: 133–146. doi:10.1016/j.rse.2005.11.016.

Chen, Y., J. Li, and X. Li. 2003. *Urban Thermal Remote Sensing: Pattern, Process, Monitor and Impact*. Beijing: Science Publisher.

Cochrane, M. A., and C. M. Souza. 1998. "Linear Mixture Model Classification of Burned Forests in the Eastern Amazon." *International Journal of Remote Sensing* 19: 3433–3440. doi:10.1080/014311698214109.

Creutzig, F., G. Baiocchi, R. Bierkandt, P. Pichler, and K. C. Seto. 2015. "Global Typology of Urban Energy Use and Potentials for an Urbanization Mitigation Wedge." *Proceedings of the National Academy of Sciences of the United States of America* 112: 6283–6288. doi:10.1073/pnas.1315545112.

Dale, V. H. 1997. "The Relationship between Land-Use Change and Climate Change." *Ecological Applications* 7: 753–769. doi:10.1890/1051-0761(1997)007[0753:TRBLUC]2.0.CO;2.

Dougherty, M., R. L. Dymond, S. J. Goetz, C. A. Jantz, and N. Goulet. 2004. "Evaluation of Impervious Surface Estimates in a Rapidly Urbanizing Watershed." *Photogrammetric Engineering and Remote Sensing* 70: 1275–1284. doi:10.14358/PERS.70.11.1275.

Foresman, T. W., S. T. A. Pickett, and W. C. Zipperer. 1997. "Methods for Spatial and Temporal Land Use and Land Cover Assessment for Urban Ecosystems and Application in the Greater Baltimore–Chesapeake Region." *Urban Ecosystems* 1: 201–216. doi:10.1023/A:1018583729727.

Gallo, K. P., A. L. McNAB, T. R. Karl, J. F. Brown, J. J. Hood, and J. D. Tarpley. 1993. "The Use of a Vegetation Index for Assessment of the Urban Heat Island Effect." *International Journal of Remote Sensing* 14: 2223–2230. doi:10.1080/01431169308954031.

Gallo, K. P., and T. W. Owen. 1999. "Satellite-Based Adjustments for the Urban Heat Island Temperature Bias." *Journal of Applied Meteorology* 38: 806–813. doi:10.1175/1520-0450(1999)038<0806:SBAFTU>2.0.CO;2.

Gao, B. C. 1996. "NDWI: A Normalized Difference Water Index for Remote Sensing of Vegetation Liquid Water from Space." *Remote Sensing of Environment* 58: 257–266. doi:10.1016/S0034-4257(96)00067-3.

Giridharan, R., S. Ganesan, and S. S. Y. Lau. 2004. "Daytime Urban Heat Island Effect in High-Rise and High-Density Residential Developments in Hong Kong." *Energy and Building* 36: 525–534. doi:10.1016/j.enbuild.2003.12.016.

Guo, G., Z. Wu, R. Xiao, Y. Chen, X. Liu, and X. Zhang. 2015. "Impacts of Urban Biophysical Composition on Land Surface Temperature in Urban Heat Island Clusters." *Landscape and Urban Planning* 135: 1–10. doi:10.1016/j.landurbplan.2014.11.007.

Gutman, G., and A. Ignatov. 1998. "The Derivation of the Green Vegetation Fraction from NOAA/AVHRR Data for Use in Numerical Models." *International Journal of Remote Sensing* 19: 1533–1543. doi:10.1080/014311698215333.

Hanamean, J. R., R. A. Pielke, C. L. Castro, D. S. Ojima, B. C. Reed, and Z. Gao. 2003. "Vegetation Greenness Impacts on Maximum and Minimum Temperatures in Northeast Colorado." *Meteorological Application* 10: 203–215. doi:10.1017/S1350482703003013.

Hart, M. A., and D. J. Sailor. 2009. "Quantifying the Influence of Land-Use and Surface Characteristicson Spatial Variability in the Urban Heat Island." *Theoretical and Applied Climatology* 95: 397–406. doi:10.1007/s00704-008-0017-5.

Hope, D., C. Gries, W. X. Zhu, W. F. Fagan, C. L. Redman, N. B. Grimm, A. L. Nelson, C. Martin, and A. Kinzig. 2003. "Socioeconomics Drive Urban Plant Diversity." *Proceedings of the National Academy of Sciences* 100: 8788–8792. doi:10.1073/pnas.1537557100.

Howard, L. 1883. *The Climate of London Deduced from Meteorological Observations*. London: Harvey and Darton.

Imhoff, M. L., P. Zhang, R. E. Wolfe, and L. Bounoua. 2010. "Remote Sensing of the Urban Heat Island Effect across Biomes in the Continental USA." *Remote Sensing of Environment* 114: 504–513. doi:10.1016/j.rse.2009.10.008.

Jenerette, G. D., S. L. Harlan, A. Brazel, N. Jones, L. Larsen, and W. L. Stefanov. 2007. "Regional Relationships between Surface Temperature, Vegetation, and Human Settlement in a Rapidly Urbanizing Ecosystem." *Landscape Ecology* 22: 353–365. doi:10.1007/s10980-006-9032-z.

Joreskog, K. G., and D. Sorbom. 1993. *LISREL 8: Structural Equation Modeling with the SIMPLIS Command Language*. Chicago, IL: Scientific Software International.

Kalnay, E., and M. Cai. 2003. "Impact of Urbanization and Land-Use Change on Climate." *Nature* 423: 528–531. doi:10.1038/nature01675.

Lamptey, B. L., E. J. Barron, and D. Pollard. 2005. "Impacts of Agriculture and Urbanization on the Climate of the Northeastern United States." *Global and Planetary Change* 49: 203–221. doi:10.1016/j.gloplacha.2005.10.001.

Landsat Project Science Office. (2002). Landsat 7 Science Data User's Handbook. Accessed 10 July 2013. http://ltpwww.gsfc.nasa.gov/IAS/handbook/handbook_toc.html.

Li, J. X., C. H. Song, L. Cao, F. G. Zhu, X. L. Meng, and J. G. Wu. 2011. "Impacts of Landscape Structure on Surface Urban Heat Islands: A Case Study of Shanghai, China." *Remote Sensing of Environment* 115: 3249–3263. doi:10.1016/j.rse.2011.07.008.

Livesley, S. J., E. G. McPherson, and C. Calfapietra. 2016. "The Urban Forest and Ecosystem Services: Impacts on Urban Water, Heat, and Pollution Cycles at the Tree, Street, and City Scale." *Journal of Environmental Quality* 45: 119–124. doi:10.2134/jeq2015.11.0567.

Lu, D., G. Li, W. Kuang, and E. Moran. 2014. "Methods to Extract Impervious Surface Areas from Satellite Images." *International Journal of Digital Earth* 7 (2): 93–112. doi:10.1080/17538947.2013.866173.

Manley, G. 1958. "On the Frequency of Snowfall in Metropolitan England." *Quarterly Journal of the Royal Meteorological Society* 84: 70–72. doi:10.1002/(ISSN)1477-870X.

Markham, B. L., and J. K. Barker. 1985. "Spectral Characteristics of the LANDSAT Thematic Mapper Sensors." *International Journal of Remote Sensing* 6: 697–716. doi:10.1080/01431168508948492.

Mathew, A., R. Chaudhary, N. Gupta, S. Khandelwal, and N. Kaul. 2015. "Study of Urban Heat Island Effect on Ahmedabad City and Its Relationship with Urbanization and Vegetation Parameters." *International Journal of Computer & Mathematical Science* 4: 2347–2357.

Oleson, K. W., A. Monaghan, O. Wilhelmi, M. Barlage, N. Brunsell, J. Feddema, L. Hu., and D. F. Steinhoff. 2015. "Interactions between Urbanization, Heat Stress, and Climate Change." *Climate Change* 129: 525–541. doi:10.1007/s10584-013-0936-8.

Pu, R., P. Gong, R. Michishita, and T. Sasagawa. 2006. "Assessment of Multi-Resolution and Multi-Sensor Data for Urban Surface Temperature Retrieval." *Remote Sensing of Environment* 104: 211–225. doi:10.1016/j.rse.2005.09.022.

Ricketts, T., and M. Imhoff. 2003. "Biodiversity, Urban Areas, and Agriculture Locating Priority Ecoregions for Conservation." *Conservation Ecology* 8 (2): 110–123. doi:10.5751/ES-00593-080201.

Rizwan, A. M., L. Y. C. Dennis, and C. Liu. 2008. "A Review on the Generation, Determination and Mitigation of Urban Heat Island." *Journal of Environmental Sciences* 20: 120–128. doi:10.1016/S1001-0742(08)60019-4.

Roberts, D. A., G. T. Batista, J. L. Pereira, E. K. Waller, and B. W. Nelson. 1998. "Change Identification Using Multitemporal Spectral Mixture Analysis: Applications in Eastern Amazonia." In *Remote Sensing Change Detection: Environmental Monitoring Methods and Application*, Eds. R. S. Lunetta and C. D. Elvidge, 137–161. Ann Arbor, MI: Ann Arbor Science.

Rogers, C. E., and J. P. McCarty. 2000. "Climate Change and Ecosystems of the Mid-Atlantic Region." *Climate Research* 14: 235–244. doi:10.3354/cr014235.

Schrijvers, P. J. C., H. J. J. Jonker, S. Kenjeres, and S. R. Roode. 2015. "Breakdown of the Night Time Urban Heat Island Energy Budget." *Building and Environment* 83: 50–64. doi:10.1016/j.buildenv.2014.08.012.

Singer, R. B., and T. B. McCord (1979). Mars: Large Scale Mixing of Bright and Dark Surface Materials and Implications for Analysis of Spectral Reflectance. In *Proceedings of 10th lunar and planetary science conference* (pp. 1835–1848). Washington DC: American Geophysical Union.

Smith, D. L., and L. Johnson. 2004. "Vegetation-Mediated Changes in Microclimate Reduce Soil Respiration as Woodlands Expand into Grasslands." *Ecology* 85: 3348–3361. doi:10.1890/03-0576.

Smith, R. M. 1986. "Comparing Traditional Methods for Selecting Class Intervals on Choropleth Maps." *Professional Geographer* 38 (1): 62–67. doi:10.1111/j.0033-0124.1986.00062.x.

Snyder, W. C., Z. Wang, Y. Zhang, and Y. Z. Feng. 1998. "Classification-Based Emissivity for Land Surface Temperature Measurement from Space." *International Journal of Remote Sensing* 19: 2753–2774. doi:10.1080/014311698214497.

Streutker, D. R. 2003. "Satellite-Measured Growth of the Urban Heat Island of Houston, Texas." *Remote Sensing of Environment* 85: 282–289. doi:10.1016/S0034-4257(03)00007-5.

Tan, J., Y. Zheng, X. Tang, C. Guo, L. Li, G. Song, X. Zhen, et al. 2010. "The Urban Heat Island and Its Impact on Heat Waves and Human Health in Shanghai." *International Journal of Biometeorology* 54: 75–84. doi:10.1007/s00484-009-0256-x.

Tang, J., L. Wang, and S. Myint. 2007. "Improving Urban Classification through Fuzzy Supervised Classification and Spectral Mixture Analysis." *International Journal of Remote Sensing* 28: 4047–4063. doi:10.1080/01431160701227687.

Tang, J., L. Wang, and Z. Yao. 2008. "Analyses of Urban Landscape Dynamics Using Multi-Temporal Satellite Images: A Comparison of Two Petroleum-Oriented Cities." *Landscape and Urban Planning* 87 (4): 269–278. doi:10.1016/j.landurbplan.2008.06.011.

Tomlinson, C. J., L. Chapman, J. E. Thornes, and C. J. Baker. 2012. "Derivation of Birmingham's Summer Surface Urban Heat Island from MODIS Satellite Images." *International Journal of Climatology* 32: 214–224. doi:10.1002/joc.v32.2.

US Census. 2011. "Population and Household." Accessed 20 September 2013 http://www.censusu.gov.

U.S. Department of Agriculture. 2015. "USDA: NRCS: Geospatial Data Gateway." Accessed June 17 2015 https://gdg.sc.egov.usda.gov/.

Viterito, A. 1989. "Changing Thermal Topography of the Baltimore-Washington Corridor: 1950-1979." *Climatic Change* 14: 89–102. doi:10.1007/BF00140177.

Von Eckardt, W., and J. Gottman. 1964. *The Challenge of Megalopolis: A Graphic Presentation of the Urbanized Northeastern Seaboard of the United States*. New York: MacMilln Press.

Voogt, J. A., and T. R. Oke. 2003. "Thermal Remote Sensing of Urban Climate." *Remote Sensing of Environment* 86: 370–384. doi:10.1016/S0034-4257(03)00079-8.

Walsh, S. J., A. Moddy, T. R. Allen, and D. G. Brown. 1997. "Scale Dependence of NDVI and Its Relationship to Mountainous Terrain." In *Scale in Remote Sensing and GIS*, Eds. D. A. Quattrochi and M. F. Goodchild, 27–55. FL: Lewis Publishers.

Wang, J., B. Huang, D. Fu, and P. M. Atkinson. 2015. "Spatiotemporal Variation in Surface Urban Heat Island Intensity and Associated Determinants across Major Chinese Cities." *Remote Sensing* 7: 3670–3689. doi:10.3390/rs70403670.

Weng, Q., D. Lu, and J. Schubring. 2004. "Estimation of Land Surface Temperature-Vegetation Abundance Relationship for Urban Heat Island Studies." *Remote Sensing of Environment* 89: 467–483. doi:10.1016/j.rse.2003.11.005.

Weng, Q., U. Rajasekar, and X. Hu. 2011. "Modeling Urban Heat Islands and Their Relationship with Impervious Surface and Vegetation Abundance by Using ASTER Images." *IEEE Transactions and Geoscience and Remote Sensing* 49: 4080–4089. doi:10.1109/TGRS.2011.2128874.

Wilby, R. L. 2008. "Constructing Climate Change Scenarios of Urban Heat Island Intensity and Ar Quality." *Environment and Planning B: Planning and Design* 35: 902–919. doi:10.1068/b33066t.

Wilson, J. S., M. Clay, E. Martin, D. Stuckey, and K. Vedder-Risch. 2003. "Evaluating Environmental Influences of Zoning in Urban Ecosystems with Remote Sensing." *Remote Sensing of Environment* 86: 303–321. doi:10.1016/S0034-4257(03)00084-1.

Wu, C., and A. T. Murray. 2003. "Estimating Impervious Surface Distribution by Spectral Mixture Analysis." *Remote Sensing of Environment* 84: 493–505. doi:10.1016/S0034-4257(02)00136-0.

Xian, G., and M. Crane. 2006. “An Analysis of Urban Thermal Characteristics and Associated Land Cover in Tampa Bay and Las Vegas Using Landsat Satellite Data.” *Remote Sensing of Environment* 104: 147–156. doi:10.1016/j.rse.2005.09.023.

Xu, H., and B. Chen. 2004. “Remote Sensing of the Urban Heat Island and Its Change in Xiamen City of SE China.” *Journal of Environment Science* 169: 276-281.

Yuan, F., and M. E. Bauer. 2007. “Comparison of Impervious Surface Area and Normalized Difference Vegetation Index as Indicators of Surface Urban Heat Island Effects in Landsat Imagery.” *Remote Sensing of Environment* 106: 375–386. doi:10.1016/j.rse.2006.09.003.

Yue, W., L. Xu, and J. Xu. 2010. “The Thermal Environment Change and Socioeconomic Driving Force in Shanghai during 1990.” *Acta Ecological Sinica* 30: 155–164.

Zhang, X., T. Zhong, and K. Wang. 2009. “Scaling of Impervious Surface Area and Vegetation as Indicators to Urban Land Surface Temperature Using Satellite Data.” *International Journal of Remote Sensing* 30: 841-859. doi:10.1080/01431160802395219.

Zhou, Y., Q. Weng, K. R. Gurney, Y. Shuai, and X. Hu. 2012. “Estimation of the Relationship between Remotely Sensed Anthropogenic Heat Discharge and Building Energy Use.” *ISPRS Journal of Photogrammetry and Remote Sensing* 67: 65–72. doi:10.1016/j.isprsjprs.2011.10.007.